

PACS numbers: 42.81.Cn; 42.70.Nq; 42.70.Gi
DOI: 10.1070/QE2007v037n04ABEH013455

Photoinduced absorption and refractive-index induction in phosphosilicate fibres by radiation at 193 nm

A.A. Rybaltovsky, V.O. Sokolov, V.G. Plotnichenko, A.V. Lanin,
S.L. Semenov, A.N. Gur'yanov, V.F. Khopin, E.M. Dianov

***Abstract*. The photoinduced room-temperature-stable increase in the refractive index by $\sim 5 \times 10^{-4}$ at a wavelength of 1.55 μm was observed in phosphosilicate fibres without their preliminary loading with molecular hydrogen. It is shown that irradiation of preliminary hydrogen-loaded fibres by an ArF laser at 193 nm enhances the efficiency of refractive-index induction by an order of magnitude. The induced-absorption spectra of preforms with a phosphosilicate glass core and optical fibres fabricated from them are studied in a broad spectral range from 150 to 5000 nm. The intense induced-absorption band (~ 800 cm^{-1}) at 180 nm is found, which strongly affects the formation of the induced refractive index. The quantum-chemical model of a defect related to this band is proposed.**

Keywords: *photosensitivity, induced absorption, fibre Bragg grating, phosphosilicate fibre*.

1. Introduction

The use of optical fibres with a phosphosilicate core instead of common germanosilicate fibres considerably simplifies the design of Raman lasers and amplifiers and enhances their efficiency. Therefore, the development of the method for writing refractive index gratings in fibres is an urgent problem requiring the study of the mechanism of photoinduced variations in the glass network caused by UV laser radiation.

It is assumed that the refractive-index induction in glasses is caused by structural transformations at the level of microscopic defects [1]. Unlike a germanosilicate glass [2], the intrinsic and photoinduced defects in a phosphosilicate glass are studied inadequately. In this paper, we study the induced absorption in a phosphosilicate glass core of preforms for drawing optical fibres and analyse the dynamics of refractive-index induction in fibres exposed to UV radiation at 193 nm.

A.A. Rybaltovsky, V.O. Sokolov, V.G. Plotnichenko, A.V. Lanin, S.L. Semenov, E.M. Dianov Fiber Optics Research Center, Russian Academy of Sciences, ul. Vavilova 38, 119991 Moscow, Russia; e-mail: andy@fo.gpi.ru, vvvl@bigfoot.com, victor@fo.gpi.ru, lanin@fo.gpi.ru, sls@fo.gpi.ru, dianov@fo.gpi.ru;
A.N. Gur'yanov, V.F. Khopin Institute of Chemistry of High-Purity Substances, Russian Academy of Sciences, ul. Tropinina 49, 603950 Nizhnii Novgorod, Russia; e-mail: tvs@ihps.nnov.ru, vkhopin@mail.ru

Received 12 October 2006
Kvantovaya Elektronika **37** (4) 388 – 392 (2007)
Translated by M.N. Sapozhnikov

2. Experimental

We studied preforms with the 12 % molar concentration of P_2O_5 in the core obtained by the MCVD method in which the core is formed by the deposition of SiO_2 and P_2O_5 particles on the internal surface of a rotating quartz tube. A single-mode fibre was drawn from a preform at temperature 1940 °C. The difference Δn of refractive indices in the fibre core and cladding at a wavelength of 633 nm was 0.011, the cut-off wavelength λ_c was 1070 nm and optical losses in the spectral range from 1100 to 1600 nm did not exceed 3 dB km^{-1}.

Absorption spectra in the 2000 – 5000-nm range were investigated for cross-section cuts of a 2-mm-thick preform core. The spectra were recorded with a Bruker IFS-113v Fourier spectrometer. The UV absorption spectra in the 150 – 350-nm range were studied for samples fabricated from the 'uncollapsed' part of a preform. The thickness of a layer doped with P_2O_5 in these samples was 70 μm. The UV absorption spectra were recorded with a McPherson VUVAS 1000 vacuum spectrophotometer.

Some samples were kept in the hydrogen atmosphere at temperature 100 °C and pressure 120 atm before UV irradiation. Fibre samples were kept in the hydrogen atmosphere for 16 h and preform cuts – for 30 days. In this way, fibres and preform cuts were preliminary loaded with molecular hydrogen H_2.

A CL-5000 ArF excimer laser (Physics Instrumentation Center, A.M. Prokhorov General Physics Institute, Troitsk) was used for excitation of samples at 193 nm. Fibres were irradiated by 8-ns, 200-mJ cm^{-2} laser pulses at a pulse repetition rate of 20 Hz.

The photoinduced refractive index was measured by two methods described in the literature. In the first method, the average value $\overline{\Delta n}_{\rm ind}$ of the refractive index induced in the fibre core was calculated by the wavelength shift $\Delta\lambda_{\rm Br}$ of the reflection peak of the Bragg grating written in the fibre [3]

$$\overline{\Delta n}_{\rm ind} = \frac{n_{\rm eff}\Delta\lambda_{\rm Br}}{\eta\lambda_{\rm Br}}, \qquad (1)$$

where $\lambda_{\rm Br}$ is the wavelength of the fibre Bragg grating (FBG) reflection maximum; $n_{\rm eff}$ is the effective refractive index for the HE_{11} mode; and η is the fraction of the HE_{11} mode energy propagating in the fibre core. Fibre Bragg gratings were produced by using a phase mask with a

period of 1068 nm, corresponding to the FBG reflection peak at ~ 1.55 μm. The measurement error of the induced refractive index was 1×10^{-5}.

The second method is based on the use of a Mach–Zehnder interferometer [4] which is produced in a fibre by writing in it two long-period gratings spaced by a distance of ~ 5 cm. The gratings were written through an amplitude mask of length 15 mm and period 300 μm, which gave rise to the interference pattern near a wavelength of 1.5 μm. The induced refractive index was calculated from the wavelength shift $\Delta\lambda$ of interference fringes measured during irradiation of the fibre by the expression

$$\Delta n_{\text{ind}} = \frac{\lambda \Delta\lambda}{L_{\text{MZ}} \Lambda_{\text{MZ}} \eta}, \qquad (2)$$

where L_{MZ} is the length of the irradiated region between gratings and Λ_{MZ} is the interference pattern period. The accuracy of measuring the shift of interference fringes was 0.1 nm, corresponding to the measurement accuracy of the induced refractive index equal to 5×10^{-6}.

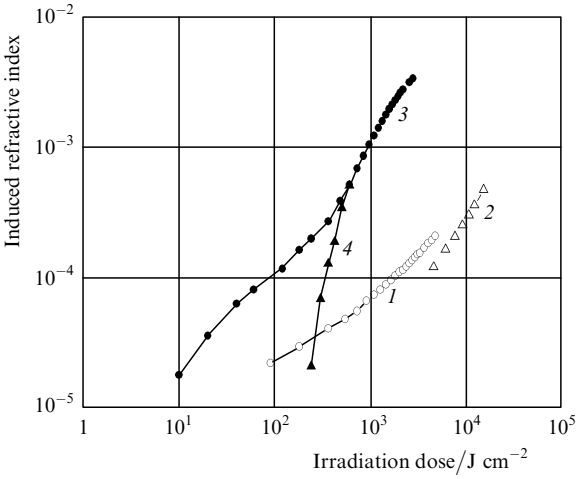

Figure 1. Dose dependences of the refractive index induced by UV radiation in a phosphosilicate glass. The induced refractive index is calculated at a wavelength of ~ 1.5 μm. The values of Δn_{ind} were measured for hydrogen-unloaded (*1*, *2*) and hydrogen-loaded (*3*, *4*) samples by using a Mach–Zehnder interferometer (*1*, *3*) and a fibre Bragg grating (*2*, *4*).

3. Results and discussion

The mechanisms of interaction of the 193-nm radiation with phosphosilicate fibres and the refractive-index induction in them by this radiation were studied in several experimental and theoretical papers [5–7]. It was shown that a phosphosilicate glass and fibres made of this glass have very low photosensitivity upon irradiation at 193 nm (the photoinduced change in the refractive index was below the detection limit, which was $\sim 10^{-6}$ in most of the experiments). In [7], the photoinduced refractive index equal to 9×10^{-6} was achieved in phosphosilicate fibres, which were fabricated by the flash condensation method [8]. However, the induced refractive index proved to be thermally unstable even at room temperature, and a FBG written in the fibre was destroyed within a few minutes.

We induced a room-temperature stable refractive index in a phosphosilicate fibre without any preliminary processing of the fibre [curves (*1*) and (*2*) in Fig. 1]. The maximum value of the photoinduced refractive index was 4.7×10^{-4} for the 15-kJ cm^{-2} radiation dose. The difference of our results on the refractive-index induction in phosphosilicate fibres from the results obtained in [7] can be explained by the difference in the structure of phosphosilicate glasses fabricated by the MCVD and flash condensation methods. Note that optical losses in phosphosilicate fibres manufactured by the latter method are considerable and achieve ~ 1000 dB km^{-1} [8]. Such high losses can appear, in particular, due to scattering caused by the phase separation of a phosphosilicate glass of the fibre core [9]. We can also assume that high losses in these fibres are related to the presence of impurities in the fibre core due to insufficient purification of initial reagents. Thus, the inhomogeneous composition of the fibre core material can significantly affect the dynamics of the refractive-index induction in fibres fabricated by the flash condensation method.

The photosensitivity of phosphosilicate glasses at 193 nm considerably increases when they are preliminary loaded with molecular hydrogen [6, 7, 10]. As follows from curves (*3*) and (*4*) in Fig. 1, the refractive index induced in a hydrogen-loaded fibre at the radiation dose $\sim 10^3$ J cm^{-2} achieves 10^{-3}, which is sufficient for producing FBGs with the reflection coefficient exceeding 99.9 %. Note that the different slope of curves (*3*) and (*4*) at comparatively low radiation doses (below 500 J cm^{-2}) is probably explained by the inadequate accuracy of determining the position of the FBG reflection peak at the initial stage of its writing. Note for comparison that the refractive index induced in a fibre without preliminary loading with hydrogen was only 7×10^{-5} at the radiation dose of 10^3 J cm^{-2}. Therefore, the photosensitivity of fibres loaded with molecular hydrogen increased in our experiments by more than an order of magnitude.

Let us analyse variations in the absorption spectra of bulk samples induced by UV radiation at 193 nm. Figure 2 shows the spectra of two samples irradiated by the same dose 1 kJ cm^{-2}.

One can see that in a sample irradiated without preliminary loading with hydrogen, a weak absorption

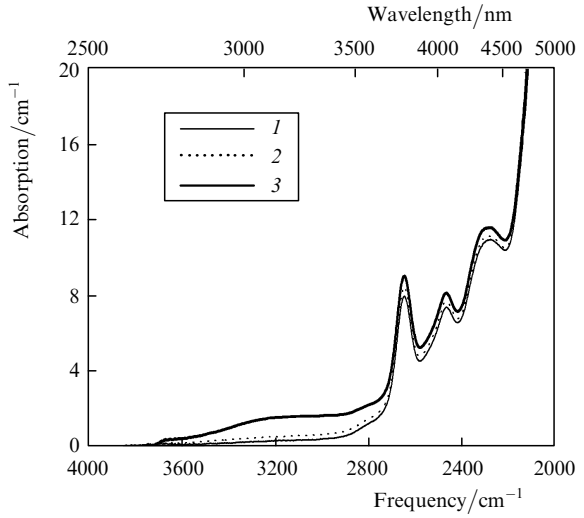

Figure 2. IR absorption spectra of the core of a phosphosilicate glass preform before (*1*), after irradiation by the 1-kJ cm^{-2} dose (*2*) and after hydrogen loading and irradiation by the 1-kJ cm^{-2} dose (*3*).

~ 0.2 cm^{-1} is induced in the 3700 – 2700-cm^{-1} range (2700 – 3700 nm). The absorption spectrum of a hydrogen-loaded sample changes stronger compared to the initial spectrum. According to [11], variations in the spectrum are caused by the induced absorption bands of hydroxyl centres: the silanol O_3Si-OH centre (the 3672-cm^{-1} band) and the $O_3Si-OH\cdots O=PO_3$ centre (the 3280-cm^{-1} band).

The maximum induced absorption was detected in the UV region. One can see from Fig. 3 that absorption induced by the 193-nm radiation in a hydrogen-loaded sample amounts to a few hundreds of cm^{-1}. This induced absorption band has a maximum at 6.9 eV (180 nm) and is also observed in the absorption spectrum of the sample before irradiation.

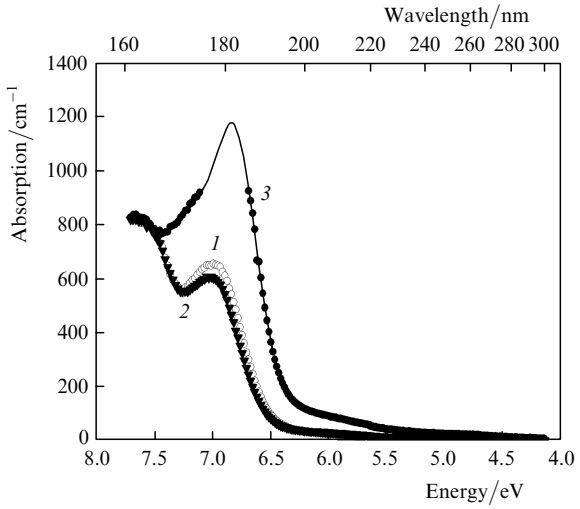

Figure 3. UV absorption spectra of the core of a phosphosilicate glass preform before (*1*), after irradiation by the 1-kJ cm^{-2} dose (*2*) and after hydrogen loading and irradiation by the 1-kJ cm^{-2} dose (*3*).

By using the method for calculating the induced refractive index from the induced absorption described in [12], we estimated the contribution of induced absorption in the 160 – 300-nm range to the induced refractive index at a wavelength of ~ 1500 nm. The calculated value of Δn_{ind} was 10^{-4}. Let us compare it with our values of the refractive index induced in the fibre (Fig. 1) and the value $n_{ind} \sim 2 \times 10^{-4}$ measured at a wavelength of 1500 nm in [13] for a preform with 12 % of P_2O_5. It seems that due to stresses produced during fibre drawing, the refractive index is induced in phosphosilicate fibres more efficiently than in samples cut from the initial preform irradiated by the same UV light. It was shown earlier for germanosilicate fibres that the use of tensile stresses during UV irradiation enhanced the efficiency of refractive-index induction approximately by a factor of five [14]. Thus, we assume that the induced UV absorption and especially the 6.9-eV absorption band observed in our experiments make a considerable contribution to Δn_{ind} in a phosphosilicate glass.

Note that the physical nature of the 6.9-eV band in a phosphosilicate band is not clear so far. The absorption band near 7 eV observed in the spectra of well-studied germanosilicate glass and pure silica is assigned, as a rule, to absorption by oxygen-deficient centres. Thus, it is assumed that the 6.9-eV absorption band in pure silica is related to the transition in the oxygen-deficient $=Si:$ centre (two-coordinated silicon atom) to the second excited singlet state [15]. In this case, the spectrum should exhibit the intense 5.1-eV absorption band corresponding to the transition to the first singlet state, which, however, is not observed in Figs 3 and 4. In [15, 16], the model of the oxygen-deficient $\equiv Si - Si \equiv$ centre (oxygen vacancy) with the 7.6-eV absorption band is also described.

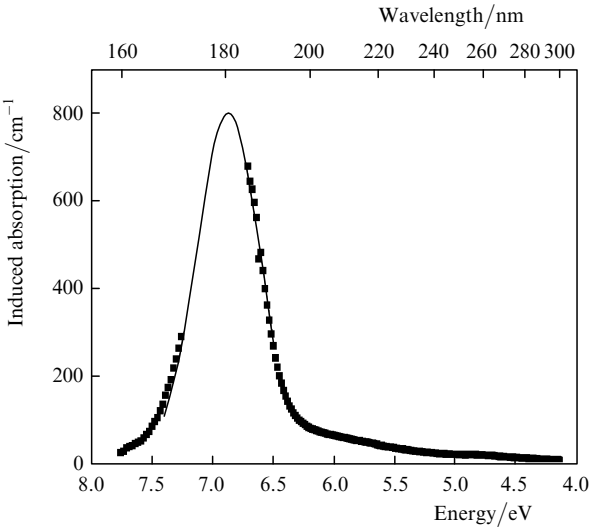

Figure 4. Induced UV absorption spectrum of the hydrogen-loaded core of a preform irradiated by the 1-kJ cm^{-2} dose.

It is reasonable to assume that the 6.9-eV absorption band observed in the spectrum of a phosphosilicate glass belongs to the oxygen-deficient defect. This assumption is indirectly confirmed by experiments on the thermal annealing of preliminarily hydrogen-loaded samples. It is known that the increase in the annealing temperature initiates thermochemical reactions between hydrogen and interatomic bonds in the glass network [17], and one of the final products of such reactions can be oxygen-deficient centres [18]. Figure 5 shows that the intensity of the 6.9-eV

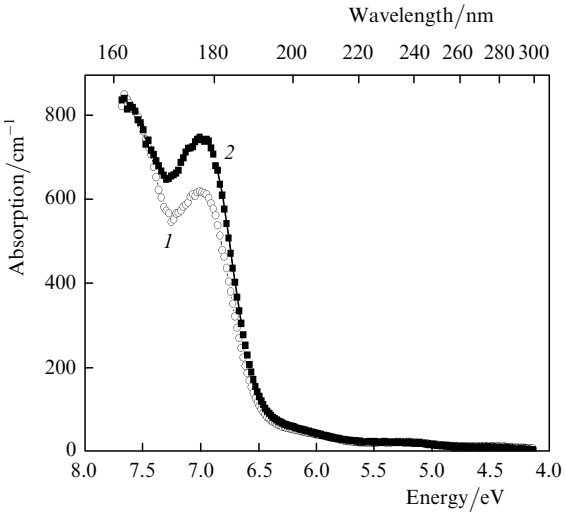

Figure 5. UV absorption spectra of the core of a hydrogen-loaded phosphosilicate glass preform (*1*) and of this preform annealed at 400 °C for 30 min (*2*).

absorption band of the hydrogen-loaded sample considerably increases after annealing of the sample at 400 °C for 30 min. The absorption band intensity increased after annealing by 130 cm^{-1}, corresponding to $\sim 20\,\%$ of the initial band intensity. The study of the thermal stability of the 6.9-eV absorption band of the hydrogen-loaded sample showed that the band intensity increased with increasing the annealing temperature up to 600 °C, while at temperatures above 600 °C the band intensity gradually decreased.

We also assume that, because the 6.9-eV band is absent in the absorption spectrum of pure silica, it belongs to an oxygen-deficient centre containing phosphorous. We propose here two models of such phosphorous oxygen-deficient centre (PODC), which are shown schematically in Fig. 6. According to our assumption, the type I PODC is a three-coordinated phosphorous atom in silica, and the type II PODC is a three-coordinated phosphorous atom bonded with a two-coordinated silicon atom in silica.

We calculated the energy of excited electronic states for both models in Fig. 6 by using the GAMESS (US) program [19]. The properties of PODC of types I and II were simulated by using the $P \equiv (O - SiO_3)_3$ and $(O - SiO_3)_3 \equiv P \cdots Si(O - SiO_3)_2$ clusters. Dangled bonds on cluster surfaces were loaded with hydrogen atoms.

We used in calculations the bases and effective core potentials proposed in [20] and [21]. The bases were additionally supplemented with polarisation functions of the d type, one for each oxygen, silicon, and phosphorous atom [$\zeta = 0.8000,\ 0.3950,\ 0.5500\ a_0^{-1}$ (a_0 is the Bohr radius), respectively]. As shown in [22] and [23], the basis chosen in this way provides good description of the properties of such systems. For hydrogen atoms, the standard 3-21G basis was used. The cluster geometry was completely optimised by the Hartree–Fock method. Once the equilibrium geometrical configuration has been obtained, we calculated the energy and oscillator strength of electronic transitions by the method of configuration interaction by using 12 one-electron levels, from which 4 levels in the electron configuration corresponding to the ground state in the Hartree–Fock method are doubly filled and 8 levels are not filled. The interaction matrix was constructed by taking into account all possible electron configurations corresponding to electronic transitions between these levels. In this case, the accuracy of calculation of the excited-state energy should be 15 % – 20 % and the oscillator strengths can be estimated by an order of magnitude. We calculated 15 lowest many-electron states.

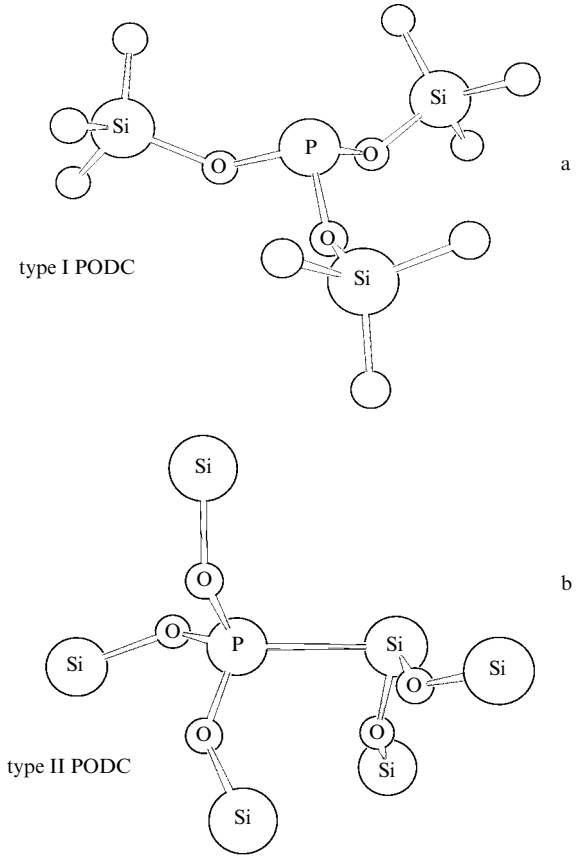

Figure 6. Structural models of the PODC: the three-coordinated phosphorous atom in silica (type I PODC) (a) and the three-coordinated phosphorous atom bonded to the two-coordinated silicon atom in silica (type II PODC) (b).

The calculation performed for the type I PODC showed that transitions from the ground state of the three-coordinated phosphorous atom to the two first excited states with energies 8.00 and 8.43 eV are allowed dipole transitions. The wavelengths of these transitions are 155 and 147 nm, and the oscillator strengths are ~ 0.3 and ~ 0.2, respectively. One can see that the calculated energies and wavelengths substantially differ from these quantities corresponding to the absorption band under study (6.9 eV or 180 nm).

The calculation performed for the type II PODC revealed better agreement with experimental data. It was found that the energies of allowed dipole transitions from the ground state of the $O_3P \cdots SiO_2$ cluster to the two first excited states were 6.82 and 6.99 eV, respectively. The wavelengths of these transitions are 182 and 177 nm, and the oscillator strengths are ~ 0.02 and ~ 0.10, respectively. These wavelengths well agree with the wavelength 180 nm of the absorption band under study. Therefore, we will assign the 6.9-eV absorption band to the transition to the excited state of the type II PODC. The distance between the three-coordinated P atom and the two-coordinated Si atom in this model of the defect is 2.53 Å, the bond order is −0.48, and the Mulliken charges of atoms P and Si are $+0.85e$ and $+0.45e$, respectively. Thus, a weakened single covalent bond is formed between atoms P and Si. On each of these atoms a nonbonding electron is localised, and the ground state of the system is a singlet state.

We assumed that the refractive-index induction in hydrogen-loaded phosphosilicate fibres is caused to a great extent by the photoinduced increase in absorption by the type II PODC. In this case, the formation of new PODCs in the phosphosilicate glass network probably occurs only when hydrogen is involved in photochemical reactions. In the core of fibres that have not been loaded preliminary with hydrogen, no new PODCs are formed and the refractive index is probably induced due to absorption by other centres, for example, phosphorous electronic centres (PECs) and phosphorous oxygen–hole centres (POHCs) [24]. The low photosensitivity detected in hydrogen-unloaded phosphosilicate fibres can be explained by a comparatively low intensity (< 10 cm^{-1}) of the absorption bands of PECs and POHCs [25].

4. Conclusions

We have observed room-temperature stable photoinduced increase in the refractive index by $\sim 5 \times 10^{-4}$ in hydrogen-unloaded phosphosilicate fibres irradiated by an ArF laser at 193 nm. It has been shown that the efficiency of refractive-index induction in hydrogen-loaded fibres irradiated at 193 nm is an order of magnitude higher.

The induced absorption spectrum of hydrogen-loaded phosphosilicate preform samples irradiated at 193 nm exhibits the intense 6.9-eV (180-nm) band. Based on the numerical simulation, the 6.9-eV band was assigned to the phosphorus oxygen-deficient centre. The quantum-chemical model of the PODC in the form of the three-coordinated phosphorous atom bonded with the two-coordinate silicon atom in silica has been proposed. It has been shown that absorption in the PODC induced by irradiation at 193 nm makes a considerable contribution to the refractive-index induction.

Acknowledgements. The authors thank E.B. Kryukova and S.E. Mosaleva for their help in experiments and useful discussions.

References

1. Hand D.P., Russell P.S.J. *Opt. Lett.*, **15**, 102 (1990).
2. Neustruev V.B. *J. Phys. Condens. Matter*, **6**, 6901 (1994).
3. Erdogan T. *J. Ligthwave Techn.*, **15** (8), 1277 (1997).
4. Dianov E.M., Vasil'ev S.A., Medvedkov O.I., Frolov A.A. *Kvantovaya Elektron.*, **24**, 805 (1997) [*Quantum Electron.*, **27**, 785 (1997)].
5. Malo B., Albert J., Bilodeau F., Kitogawa T., Johnson D.C., Hill K.O., Hattory K., Hibino Y., Gujrathi S. *Appl. Phys. Lett.*, **65** (4), 394 (1994).
6. Strasser T.A., White A.E., Yan M.F., Lemaire P.J., Erdogan T. *Proc. Conf. 'Optical Fiber Communications' (OFC'95)* (San Diego, CA, USA, 1995) Vol. WN2, p. 159.
7. Canning J., Inglis H.G. *Opt. Lett.*, **20** (21), 2189 (1995).
8. Carter A.L., Poole S.B., Sceats M.G. *Electron. Lett.*, **28** (21), 2009 (1992).
9. Carter A.L., Sceats M.G., Poole S.B., Hanna J.V. *Proc. Conf. 'Optical Fiber Communications' (OFC'94)* (San Jose, CA, USA, 1994) p. 4.
10. Larionov Yu.V., Rybaltovsky A.A., Semenov S.L., Bubnov M.M., Dianov E.M. *Kvantovaya Elektron.*, **32**, 124 (2002) [*Quantum Electron.*, **32**, 124 (2002)].
11. Plotnichenko V.G., Sokolov V.O., Kryukova E.B., Dianov E.M. *J. Non-Crystall. Sol.*, **270**, 20 (2000).
12. Leconte B., Xie W.X., Douay M., Bernage P., Niay P., Bayon J.F., Delevaque E., Poignant H. *Proc. Conf. 'Bragg Gratings, Photosensitivity and Poling in Glass Fibers and Waveguides' (BGPP'97)* (Williamsburg, Virginia, USA, 1997) Vol. 17, p. 169.
13. Butov O.V., Golant K.M., Tomashuk A.L. *Proc. XIX Intern. Cong. on Glass* (Edinburgh, Scotland, Great Britain, 2001) Vol. 2, p. 53.
14. Salik E., Starodubov D.S., Feinberg J. *Opt. Lett.*, **25** (16), 1147 (2000).
15. Skuja L. *J. Non-Crystall. Sol.*, **239**, 16 (2000).
16. Pacchioni G. *Proc. Conf. 'NATO Advanced Study Institute on Defects in SiO_2 and related dielectrics: Science and Technology'* (Erice, Italy, 2000) Vol. 2, p. 161.
17. Lanin A.V., Golant K.M., Nikolin I.V. *Zh. Tekh. Fiz.*, **68**, 61 (2004).
18. Awazu K., Kawazoe H., Yamane M. *J. Appl. Phys.*, **68** (6), 2713 (1990).
19. Schmidt M.W., Baldridge K.K., Boatz J.A., Elbert S.T., Gordon M.S., Jensen J.J., Koseki S., Matsunaga N., Nguyen K.A., Windus T.L., Dupuis M., Montgomery J.A. *J. Comput. Chem.*, **14**, 1347 (1993).
20. Stevens W.J., Balsch H., Krauss M. *J. Chem. Phys.*, **81** (12), 6026 (1984).
21. Gundary T.R., Stevens W.J. *J. Chem. Phys.*, **98** (7), 5555 (1993).
22. Amado A.M., Ribeiro-Claro P.J.A. *J. Mol. Struct. (THEOCHEM)*, **469** (1–3), 191 (1999).
23. Ribeiro-Claro P.J.A., Amado A.M. *J. Mol. Struct. (THEOCHEM)*, **528** (1–3), 19 (2000).
24. Hosono H., Kajihara K., Hirano M., Oto M. *J. Appl. Phys.*, **91** (7), 4121 (2002).
25. Larionov Yu.V., Rybaltovsky A.A., Semenov S.L., Kurzanov M.A., Obidin A.Z., Vartapetov S.K. *Kvantovaya Elektron.*, **33**, 919 (2003) [*Quantum Electron.*, **33**, 919 (2003)].